Journal of Oleo Science
Copyright ©2015 by Japan Oil Chemists' Society
doi : 10.5650/jos.ess14170
J. Oleo Sci. **64**, *(3) 337-346 (2015)*

JOURNAL OF OLEO SCIENCE
Jos

Topical Therapies for Rheumatoid Arthritis by Gel Ointments containing Indomethacin Nanoparticles in Adjuvant-Induced Arthritis Rat

Noriaki Nagai, Chiaki Yoshioka and Yoshimasa Ito*

Faculty of Pharmacy, Kinki University, 3-4-1 Kowakae, Higashi-Osaka, Osaka, 577-8502, Japan

Abstract: Indomethacin (IMC), a nonsteroidal anti-inflammatory drug, has been used in the treatment of rheumatoid arthritis (RA), although its clinical use has been limited by its systemic side effects that include gastrointestinal lesions. Therefore, the development of IMC formulations that do not cause gastrointestinal lesions is highly anticipated. In this study, we designed new topical formulations containing IMC solid nanoparticles (IMC_{nano} gel ointment), and investigated their pharmacokinetics. In addition, we demonstrate the preventive effects of this topical application of IMC nanoparticles on inflammation in adjuvant-induced arthritis rat (AA rat). The IMC_{nano} gel ointment was prepared using Bead Smash 12 (a bead mill) and additives including 2-hydroxypropyl-β-cyclodextrin, methylcellulose and Carbopol 934; the mean particle size of the IMC nanoparticles was 173 ± 91 nm (means ± S.D.). The application of the IMC_{nano} gel ointment attenuated the increase in paw edema of the hind feet of AA rats in comparison with AA rats treated with gel ointment containing IMC microparticles (IMC_{micro} gel ointment, particle diameter 17.1 ± 11.6 μm, means ± S.D). In addition, the accumulation of IMC from the IMC_{nano} gel ointment in skin tissue was significantly large than for the IMC_{micro} gel ointment; however, the plasma IMC concentrations were similar for the IMC_{micro} and IMC_{nano} gel ointments. Our findings suggest that the dermal application of nanoparticles may enable a medication to be applied without high-systemic drug levels, which could provide efficient and effective therapy that spares patients from unwanted side effects. A formulation of a topical drug delivery system using IMC nanoparticles may provide a delivery option for the clinical treatment of RA.

Key words: nanoparticle, indomethacin, gel ointment, topical drug delivery, adjuvant-induced arthritis

1 INTRODUCTION

Rheumatoid arthritis (RA) is a complex chronic inflammatory disease dependent on multiple interacting environmental and genetic factors, which make it difficult to understand its pathogenesis and thereby to find effective therapies[1]. In treatments for RA, the focus is on the reduction of pain, inflammation and joint damage. The principal pharmacological agents are nonsteroidal anti-inflammatory drugs (NSAIDs), disease-modifying anti-rheumatic drugs, glucocorticoids and specific inhibitors of the mediator response[2]. Indomethacin (IMC), a NSAID, is widely used in the management of patients affected by dermatitis and RA[3]. Oral therapy with IMC is very effective, but its clinical use is often limited by its significant side effects[4-9] that include irritation and ulceration of the gastrointestinal mucosa. Also, it requires frequent dosing[10]. In addition, it is known that RA patients taking IMC are more susceptible to IMC-induced gastrointestinal lesions in comparison with other patients[4-8, 11]. Due to these problems, several studies are aimed at the development of an efficient means to allow for topical IMC administration in order to increase local soft-tissue and joint concentrations by reducing the systemic distribution so as to limit the harmful side-effects[12, 13].

Dermal application offers many advantages over conventional oral delivery for medications such as allowing smooth and continuous drug delivery and reduced the maximum plasma concentration of the drug (C_{max}). Dermal systems improve the tolerability profile and permit the achievement of relatively high local drug concentrations without systemic side effects. However, the amount of drug that can be administered transdermally is quite low since transdermal delivery is severely limited by the inability of a large majority of drugs to cross the skin at therapeutic rates due

*Correspondence to: Yoshimasa Ito, Faculty of Pharmacy, Kinki University, 3-4-1 Kowakae, Higashi-Osaka, Osaka, 577-8502, Japan.
E-mail: itoyoshi@phar.kindai.ac.jp
Accepted October 21, 2014 (received for review August 1, 2014)
Journal of Oleo Science ISSN 1345-8957 print / ISSN 1347-3352 online
http://www.jstage.jst.go.jp/browse/jos/ http://mc.manusriptcentral.com/jjocs

to the barrier imposed by the outer stratum corneum layer of the skin. Accordingly, considerable research efforts are focused on drug permeation, and various enhancing methods have been tried: iontophoresis and electroporation[14, 15], phonophoresis[16, 17], chemical methods and absorption enhancers[18, 19]. Recently, strategies using micro/nanoparticles have been developed and investigated. Nanoparticles can be engineered to carry drug payloads, image contrast agents, or gene therapeutics for diagnosing and treating disease, with cancer being a primary focus, and research into nanomedicines has increased enormously during the past years[20−28]. The size of a particle influences its functionality in terms of uptake, residence in circulation, adherence, degradation, as well as clearance[29−33]. The fate of particles inside the body has been reported as follows[34]: ≧2 μm, trapped inside liver cells; ≧300 - 400 nm, captured by macrophages and excreted; ≧200 nm, filtered in the spleen; ≦100 nm, escape from blood vessels through the endothelial lining. Thus, size governs the movement of nanoparticles inside tissues. We also reported that a dermal application using these nanoparticles enhanced drug permeability through the skin[35]. It is expected that drug systems using nanoparticles may provide an alternative strategy for increasing drug permeation[36−39], and it is possible that a topical drug delivery system using nanoparticles may lead to an expansion of their usage as therapy for RA patients.

Here, we have designed new topical formulations containing IMC solid nanoparticles, and investigated their pharmacokinetics. In addition, we demonstrate the preventive effects of these IMC nanoparticle formulations on inflammation in adjuvant-induced arthritis (AA) rats.

2 EXPERIMENTAL

2.1 Animals and reagents

Male Wistar rats, aged 7 weeks, and Dark Agouti (DA) rats, aged 6 to 13 weeks, were housed under standard conditions (12 h/d fluorescent light (07:00-19:00), 25℃ room temperature), and allowed free access to a commercial diet (CE-2, Clea Japan Inc., Tokyo, Japan) and water. 2-Hydroxypropyl-β-cyclodextrin (HPβCD, average molar substitution, 0.6; average MW, 1380) was purchased from Nihon Shokuhin Kako Co., Ltd. (Tokyo, Japan). Low-substituted methylcellulose (MC, METOLOSE SM-4, average viscosity, 4 Pa·s at 20℃) was provided by Shin-Etsu Chemical Co., Ltd. (Tokyo, Japan). Carboxypolymethylene (Carbopol® 934) was obtained from Serva (Heidelberg, Germany). Conventional IMC (solid, IMC microparticles, 17.1 ± 11.6 μm, means ± S.D.) was purchased from Wako Pure Chemical Industries, Ltd. (Osaka, Japan). All other chemicals used were of the highest purity commercially available.

2.2 Preparation of gel ointment containing IMC nanoparticles

Carbopol® 934 was added to distilled water, allowed to swell for 1 h at room temperature, and neutralized with 5% ammonia water (gel base). IMC nanoparticles were prepared using zirconia beads and Bead Smash 12 (a bead mill, Wakenyaku Co. Ltd, Kyoto, Japan)[35, 40−42]. Zirconia beads (diameter: 2 mm) were added to the IMC microparticles with MC, and the mixtures were crushed with the Bead Smash 12 for 30 sec (3,000 rpm, 4℃). The mixtures were then dispersed in saline with 5% HPβCD, and crushed again with the Bead Smash 12 (5,500 rpm, 30 sec × 15 times, 4℃) in the presence of zirconia beads (diameter: 0.1 mm). The particle size of milled IMC was 0.173 ± 0.091 μm (means ± S.D.), and the solubility of IMC in saline with and without 5% HPβCD was 0.003% and 0.012%, respectively (the inclusion complex by 5% HPβCD was 0.009%). After milling, the IMC nanoparticles containing HPβCD and MC were added to the Carbopol® 934 gel base, and stirred until the mixture became uniform (IMC_{nano} gel ointment). The gel ointment containing IMC microparticles was prepared by adding IMC microparticles, HPβCD and MC into the Carbopol® 934 gel base (IMC_{micro} gel ointment). The formulation of the gel ointment containing IMC is as follows: 1% IMC, 5% HPβCD, 0.5% MC, 3% Carbopol® 934, w/w%. The dispersity of the nanoparticles in the ointment base was confirmed as follows : 1% IMC_{micro} and IMC_{nano} gel ointments were divided into 10 parts, and the IMC concentration in each part was measured by HPLC (IMC_{micro}, 0.99 ± 0.11; IMC_{nano}, 1.05 ± 0.06, %, means ± S.E., n = 10). Figure 1 shows the particle size of the 1% IMC_{micro} and IMC_{nano} gel ointments. The particle size was measured using a nanoparticle size analyzer SALD-7100 (Shimadzu Corp., Kyoto, Japan; refractive index 1.60-0.10i). The IMC_{micro} and IMC_{nano} gel ointments were stable for one month after preparation (mean particle size: IMC_{micro}, 17.8 ± 12.6; IMC_{nano}, 0.191 ± 0.105, μm, means ± S.D.), and no decrease in IMC concentration in the IMC_{micro} or IMC_{nano} gel ointments was observed during the one month.

2.3 Release of IMC from IMC gel ointments

An experiment was carried out using 100 and 450 nm pore size membrane filters (MF™-MEMBRANE FILRER, Merck Millipore, Tokyo, Japan) and a Franz diffusion cell[35, 43]. The donor side of the membrane filter was soaked in buffer (0.85% NaCl-10 mM phosphate buffer, pH 7.4) for 12 h at 4℃ to equilibrate the membrane. Then 0.3 g IMC gel ointment was spread uniformly over the membrane, which was then mounted in the Franz diffusion cell (reservoir volume 12.2 ml, 1.6 cm i.d. *O*-ring flange), and occluded with aluminium foil. The diffusion cells were thermoregulated in a water bath at 37℃ for 24 h. One hundred microliter aliquots of sample solution were withdrawn from the reservoir chamber at the indicated time intervals and replaced

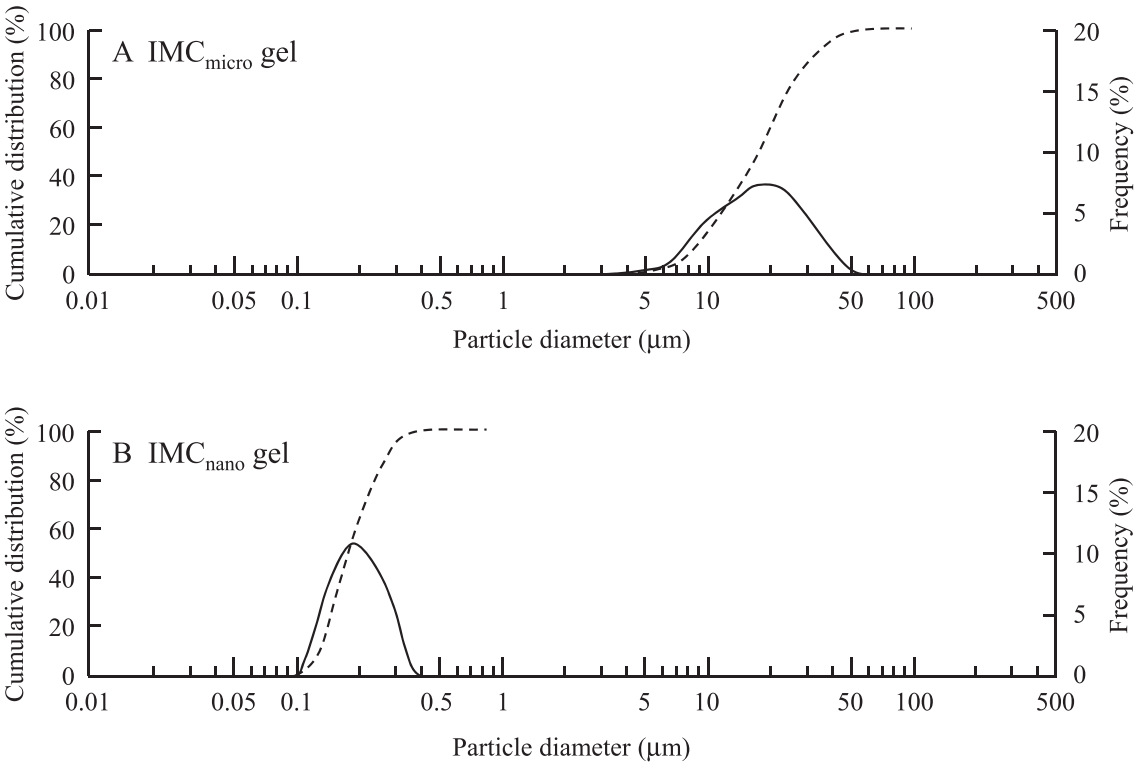

Fig. 1 Cumulative Particle Size Distribution and Frequency of 1% IMC$_{micro}$ (A) and IMC$_{nano}$ (B) Gel Ointments.
Gel ointments were dispersed in water, and the particle sizes were determined using a nanoparticle size analyzer SALD-7100 (refractive index 1.60-0.10i). Mean particle size: IMC$_{micro}$ gel ointment, 17.5 ± 12.0; IMC$_{nano}$ gel ointment, 0.186 ± 0.101, μm, means ± S.D.

with the same volume of buffer. Ten microliters of filtrate was added to 100 μl methanol containing 0.1 μg propyl p-hydroxybenzoate (internal standard), and the mixture was filtered through a Chromatodisk 4A (pore size 0.45 μm, Kurabo Industries Ltd., Osaka, Japan). The filtered solution (10 μl) was injected into an Inertsil® ODS-3 (3 μm, column size: 2.1 mm × 50 mm) column (GL Science Co., Inc., Tokyo, Japan) on a Shimadzu LC-20AT system equipped with a column oven CTO-20A (Shimadzu Corp., Kyoto, Japan). The mobile phase consisted of acetonitrile/50 mM acetic acid (40/60, v/v) at a flow rate of 0.25 mL/min; the column temperature was 35℃, and the wavelength for detection was 254 nm.

2.4 *In vitro* skin penetration of IMC$_{micro}$ and IMC$_{nano}$ gel ointments

The *in vitro* skin penetration experiment was carried out using the Franz diffusion cell[35, 43]. On the day before the experiment, the hair on the abdominal area of 7 week-old Wistar rats was carefully removed with an electric clipper and electric razor. The following day, pieces (3 × 3 cm area) of full-thickness abdominal skin were excised from the rats, and the adherent fat and other visceral debris were removed from the undersurface. The dermal side of the full-thickness skin was soaked in buffer (0.85% NaCl-10 mM phosphate buffer, pH 7.4) for 12 h at 4℃ to equilibrate the skin. Then 0.3 g IMC gel ointment was uniformly spread over the stratum corneum of the skin, which was then mounted in a Franz diffusion cell (reservoir volume 12.2 ml, 1.6 cm i.d. *O*-ring flange), and occluded with aluminium foil. The diffusion cells were thermoregulated in a water bath at 37℃ for 30 h. The IMC concentrations in the samples were determined by the HPLC method described above. The data obtained were analyzed using the following formula (Eqs. 1-3)[35, 44]:

$$t_{lag} = \frac{\delta^2}{6D} \quad \text{Eq. 1}$$

$$J_c = \frac{K_m \cdot D \cdot C_{IMC}}{\delta} = K_p \cdot C_{IMC} \quad \text{Eq. 2}$$

$$Q_t = J_c \cdot A \cdot (t - t_{lag}) \quad \text{Eq. 3}$$

where J_c is the IMC penetration rate, K_m is the skin/preparation partition coefficient, D is the diffusion constant within the skin, t_{lag} is the lag time, δ is thickness of the skin (0.071 cm, average for 5 rats), Q_t is the total amount of IMC appearing in the reservoir solution at time t, and A is the effective area of skin (2 cm^2); J_c and t_{lag} were estimated by fitting each penetration profile to Eq. 3. The penetration coefficient through the skin, K_p, is given by J_c/C_{IMC}. A non-linear least-squares computer program (MULTI) was em-

ployed for the calculation[45].

2.5 *In vivo* percutaneous absorption of IMC_{micro} and IMC_{nano} gel ointments

On the day before the experiment, the hair on the abdominal area of 7 week-old Wistar rats was carefully removed with an electric clipper and electric razor, and a cannula filled with 30 μg/ml heparin (silicone tubing; I.D., 0.5 mm, O.D., 1.0 mm) was inserted into the right jugular vein under isoflurane anesthesia. 0.3 g of IMC gel ointment was fixed on the shaved abdominal skin with an adhesive and immediately occluded with adhesive tape. At 24 h after the start of the experiment, the skin surface to which the gel ointment was applied was washed with saline, and the IMC gel ointments were reapplied. Venous blood (200 μl) was collected at 0-96 h after the application of IMC gel ointment from the jugular vein through the cannula. The blood was centrifuged at 3,000 rpm for 20 min at 4℃, and the plasma obtained was stored at −80℃ until IMC analysis. The IMC concentrations in the samples were determined by the HPLC method described above. The IMC concentration in the plasma after a single injection of 0.3 ml of IMC solution (200 μg/kg) into the femoral vein was analyzed according to Eq. 4[35]:

$$C_{IMC} = C_0 \cdot e^{-k_e \cdot t} \quad \text{Eq. 4}$$

where C_{IMC} is IMC concentration in the plasma, C_0 is the initial concentration of IMC in the plasma (2.68 ± 0.13 μg/ml), k_e is the elimination rate constant for IMC from the plasma. The k_e and distribution volume (V_d) data obtained from 5 experiments were 0.05 ± 0.07 h^{-1} and 52.1 ± 1.98 ml/kg, respectively.

The absorption of IMC after a single administration of IMC gel ointment was calculated as the apparent absorption rate constant (k_a, h^{-1}) according to Eq. 5[35]:

$$C_{IMC} = \frac{k_a \cdot F \cdot D}{V_d (k_a - k_e)} (e^{-k_e \cdot (t - t_{lag})} + e^{-k_a \cdot (t - t_{lag})}) \quad \text{Eq. 5}$$

where C_{IMC} is the IMC concentration in the plasma, D is the dose of IMC administered (1% gel ointments, 0.3 g), k_a is the absorption rate constant, t is time (0-24 h) after IMC administration, t_{lag} is lag time (h), V_d is the distribution volume, F is the fraction of IMC absorbed. In addition, the plasma IMC concentration data after repeated administration of IMC gel ointments (0.3 g/day, interval 24 h) were estimated by Eq. 6[35]

$$C_{IMC} = \frac{k_a \cdot F \cdot D}{V_d (k_a - k_e)} \cdot \left[\left(\frac{1 - e^{-N \cdot k_e \cdot \tau}}{1 - e^{-k_e \cdot \tau}} \right) e^{-k_e \cdot t} - \left(\frac{1 - e^{-N \cdot k_e \cdot \tau}}{1 - e^{-k_e \cdot \tau}} \right) e^{-k_e \cdot t} \right] \quad \text{Eq. 6}$$

where τ is the interval after IMC administration (24 h), N is the frequency of IMC administration. A nonlinear least-squares computer program (MULTI) was employed for these calculation (Eqs. 4-6).

The area under the IMC concentration-time curve ($AUC_{0\text{-}24h}$) was analyzed according to the following equation (Eq. 7):

$$AUC_{0\text{-}24h} = \int_{0h}^{24h} C_{IMC} dt \quad \text{Eq. 7}$$

Briefly, $AUC_{0\text{-}24h}$ was determined according to the trapezoidal rule up to 24 h, which was the time of the final IMC concentration measurement.

2.6 Accumulation of IMC_{micro} and IMC_{nano} gel ointments in skin tissue

On the day before the experiment, the hair on the abdominal area of 7 week-old Wistar rats was carefully removed with an electric clipper and electric razor. The following day, 0.3 g of IMC gel ointment was fixed on the shaved abdominal skin with an adhesive and immediately occluded with adhesive tape. At 24 h after the start of the experiment, the skin surface to which the gel ointment was applied was washed with saline, and the IMC gel ointments were reapplied. The gel ointment on the skin surface was wiped off with an Elleair Prowipe Soft Micro Wiper S220 (Prowipe, DAIO PAPER CORPORATION, Tokyo, Japan) soaked in saline, and pieces (2 cm^2) of abdominal skin to which the IMC gel ointments were applied were excised at 0-24 h after application. The adherent fat and other visceral debris were removed from the undersurface, and the skin samples obtained were stored at -80℃ until IMC analysis. The frozen skin was homogenized in methanol using a Physcotron homogenizer (MICROTEC CO., LTD., Chiba, Japan). The homogenates were centrifuged at 15,000 rpm for 20 min at 4℃, and the supernatants were used for the measurement of IMC. The IMC concentrations in the samples were determined by the HPLC method described above.

2.7 Application of IMC gel ointments to AA rats

Arthritis was induced by the injection of 50 μl of adjuvant, a suspension of 10 mg/ml heat-killed *Mycobacterium butyricum* (Difco, Detroit, MI) in Bayol F oil, into the plantar region of the right hind foot and tail of DA rats. The control group received 50 μl of Bayol F oil alone. The rats were hooded to prevent them from licking, and 0.3 g of IMC gel ointment was applied to the right foot daily (9:00). When reapplying the gel ointment, the old gel ointment on the skin surface was first wiped off with saline on a Prowipe. The application of IMC gel ointments was started after adjuvant injection. In this study, inflammation during the development of AA was assessed by measuring paw volume (paw edema), a parameter of inflammation, by plethysmometry. In this paper, the inflammatory scores are represented as AUC (the area under the paw volume-time curve, $AUC_{0\text{-}42d}$). The values of $AUC_{0\text{-}42d}$ were calculated according to the following equation (Eq. 8):

$$AUC_{14\text{-}42d} = \int_{14d}^{42d} V dt \quad \text{Eq. 8}$$

where V and t are the paw volume and the number of days

after adjuvant injection, respectively.

2.8 Statistical analysis

All values are represented as mean ± standard error of the mean (S.E.). Unpaired Student's or Aspin-Welch's *t*-tests were used to determine statistical difference, and multiple groups were evaluated by one-way analysis of variance (ANOVA) followed by Dunnett's multiple comparison. *P* values less than 0.05 were considered significant.

3 RESULTS AND DISCUSSION

3.1 Percutaneous Penetration of IMC Released from IMC_{micro} and IMC_{nano} Gel Ointments

First, we prepared IMC nanoparticles. Additives are very important in the preparation of high quality nanomedicines since they affect the environment around the surface of the particles. In a previous study, we found that the addition of HPβCD and MC was suitable for the preparation of nanoparticles using mill methods[35, 40–42]. HPβCD is a cyclic oligosaccharide with a hydrophilic outer surface and a lipophilic cavity in its center. It is capable of forming inclusion complexes with many lipophilic drugs by taking up the drug molecule, or part of it, into the lipophilic cavity[46, 47]. Moreover, HPβCD enhances the stability of drug dispersions containing nanoparticles by attaching to the surface of the nanoparticles[35, 40–42]. MC is a water-soluble substance with a high degree of purity, uniformity and transparency. MC solutions are neutral, odorless, and tasteless, and are also stable over a wide pH range. We have reported that MC is needed to prepare drug nanoparticles by the bead mill method[35, 40–42]. Therefore, the IMC nanoparticles were prepared using additives (HPβCD and MC) and Bead Smash 12, which resulted in the preparation of high quality IMC nanoparticles (particle size, 173 ± 91 nm, means ± S.D.). The data indicate that the milled IMC nanoparticles are homogeneous with a narrow particle size distribution. Clinically, ointments, creams and gels are used in formulations for dermal application, and gels are particularly used pharmaceutically as lubricants as well as carriers for many drugs to provide a local effect and percutaneous absorption[48, 49]. Therefore, a gel ointment containing IMC nanoparticles was prepared using Carbopol 934, which has excellent thickening, emulsifying and gelling properties, allowing the uniform incorporation of the IMC nanoparticles (Fig. 1). The IMC_{micro} and IMC_{nano} gel ointments were stable for one month after preparation (mean particle size: IMC_{micro}, 17.8 ± 12.6; IMC_{nano}, 0.191 ± 0.105, μm, means ± S.D.), with no decrease in IMC concentration in either ointment observed during the one month. These results show that the procedures developed in this study are suitable for the preparation of gel ointments containing IMC nanoparticles.

Next, the drug release and skin penetration of IMC_{micro} and IMC_{nano} gel ointments was demonstrated. Figure 2 shows the penetration profiles of IMC through a membrane filter after the application of IMC_{micro} and IMC_{nano} gel ointments. Although the IMC release from the IMC_{nano} gel ointment was similar to that from the IMC_{micro} gel ointment in experiments using 100 nm pore size membranes, the IMC penetration profile of the IMC_{nano} gel ointment through a 450 nm pore size membrane was significantly higher than that of the IMC_{micro} gel ointment, and the release from the IMC_{micro} gel ointment was 38.9% of that from the IMC_{nano} gel ointment 24 h after the application of 1% IMC gel ointment. This result suggests that the IMC emitted from the IMC_{nano} gel ointment remains in the state of IMC nanoparticles.

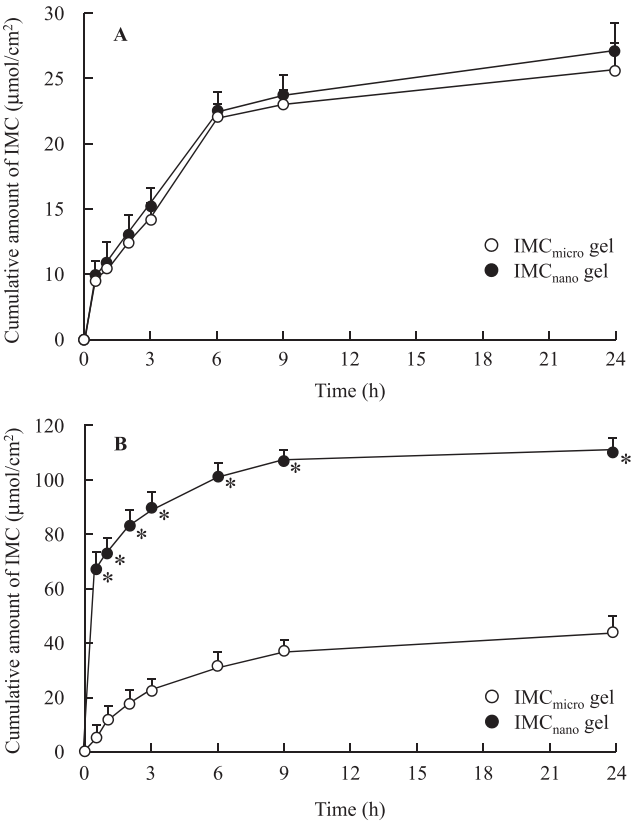

Fig. 2 Release of IMC from Gel Ointments containing IMC Nanoparticles through 100 nm (A) and 450 nm (B) Pore Size Membrane.
0.3 g of IMC gel ointment containing micro- (open circles) or nanoparticles (closed circles) was applied to 100 nm (A) and 450 nm (B) pore size membranes for 0-24 h. The data represent the means ± S.E. of 6 independent experiments. *$p < 0.05$ vs. IMC_{micro} gel ointment for each category.

Figure 3 shows the penetration profiles of IMC through rat skin after the application of IMC_{micro} and IMC_{nano} gel ointments, and Fig. 4 shows the absorption profiles of IMC

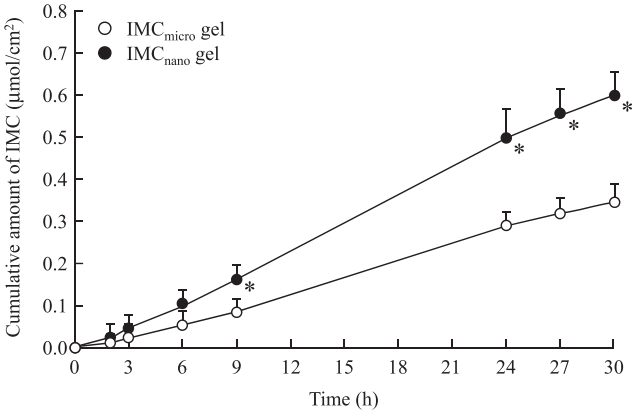

Fig. 3 In Vitro Skin Penetration of IMC Released from IMC$_{micro}$ and IMC$_{nano}$ Gel Ointments.
0.3 g of IMC gel ointment containing micro- (open circles) or nanoparticles (closed symbols) was applied to abdominal skin pieces for 0-30 h. The data represent the means ± S.E. of 6 rat skins. *$p < 0.05$ vs. IMC$_{micro}$ gel ointment.

through rat skin following the applications of IMC$_{micro}$ and IMC$_{nano}$ gel ointments. Table 1 and 2 summarize the pharmacokinetic parameters calculated from the in vitro skin penetration data (Table 1) and the *in vivo* percutaneous absorption data (Table 2). In the *in vitro* rat skin penetration experiments, the amounts of IMC that penetrated the skin increased linearly in the case of both IMC gel ointments up to 30 h after the application of the gel ointment (Fig. 3). Therefore, we used data collected in the 0 - 30 h range to calculate the pharmacokinetic parameters (Table 1). The amount of penetrated IMC, the penetration rate (J_c), penetration coefficient through the skin (K_p) and skin/preparation partition coefficient (K_m) values of the IMC$_{nano}$ gel ointment were all significantly higher than those of the IMC$_{micro}$ gel ointment. The diffusion constant within the skin (D) and lag time (t_{lag}) for the IMC$_{micro}$ and IMC$_{nano}$ gel ointments showed no significant difference. However, the absorption profiles of IMC through the skin following the applications of IMC$_{micro}$ and IMC$_{nano}$ gel ointments were similar (Fig. 4A and Table 2), and the IMC plasma concentration following the repetitive administration of the IMC$_{micro}$ or IMC$_{nano}$ gel ointments reached a plateau at 48-96 h with a value of 1.4 - 3.0 μg/ml (concentration at steady state, C_{ss}, Fig. 4). On the other hand, the IMC concentrations in the skin tissue of rats receiving the IMC$_{nano}$ gel ointment were significantly higher than those of rats receiving the IMC$_{micro}$ gel ointment (Fig. 5). We show that the supply of IMC from the IMC$_{nano}$ gel ointment was higher than that from IMC$_{micro}$ gel ointment in this study (Figs. 2 and 3). Therefore, the greater amount of IMC from the IMC$_{nano}$ gel ointment may be related to the IMC concentrations in the skin tissue, and the IMC in skin may show only a limited shift to the blood.

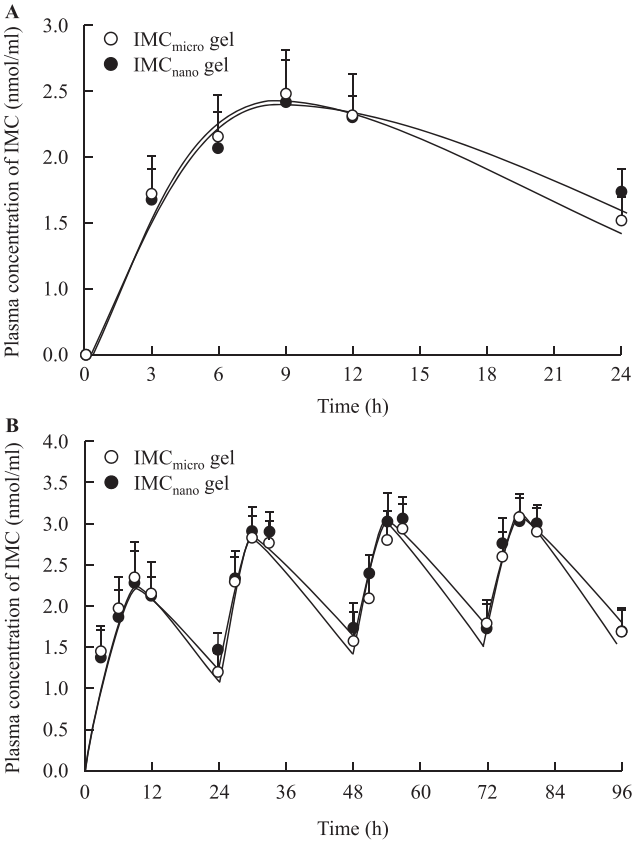

Fig. 4 Changes in Plasma IMC Concentration after the Application of IMC$_{micro}$ and IMC$_{nano}$ Gel Ointments.
0.3 g of 1% IMC gel ointment containing micro- (open circles) or nanoparticles (closed circles) was applied to the abdominal skin of rats for 0-96 h. A; plasma concentration of IMC after a single application of IMC gel ointment for 0-24 h, B; plasma concentration of IMC after repetitive application of IMC gel ointment for 0-96 h. The plasma IMC concentration data after the repetitive application of IMC gel ointments (0.3 g/day, interval 24 h) were estimated according to Eqs. 4-6. Solid lines represent the fitted curves for multiple applications of 1% IMC gel ointment containing micro- or nanoparticles. The data represent the means ± S.E. of 6 rats.

These results show that the characteristics of the IMC$_{micro}$ and IMC$_{nano}$ gel ointments in skin differ. In addition, we demonstrated the plasma concentration and accumulation in the skin following the application of a commercially available IMC gel ointment (IDOMETHINE$_{KOWA}$ gel 1%). The plasma concentration following the repetitive administration of IMC$_{nano}$ gel ointment was lower than that following the commercially available ointment (C_{ss}, 10.3 - 22.9 μg/

Table 1 Pharmacokinetic Parameters for the *In Vitro* Skin Penetration of IMC Released from 1% IMC_{micro} and IMC_{nano} Gel Ointments.

Ointment	J_c (μmol/cm^2/h)	K_p ($\times 10^{-4}$ cm/h)	K_m	t_{lag} (h)	D ($\times 10^{-4}$ cm^2/h)
IMC_{micro} gel	9.02 ± 0.40	0.90 ± 0.39	0.14 ± 0.06	1.89 ± 0.05	0.44 ± 0.02
IMC_{nano} gel	24.8 ± 0.47*	2.49 ± 0.40*	0.37 ± 0.05*	1.80 ± 0.06	0.47 ± 0.02

The experiments were carried out using a Franz diffusion cell; the pharmacokinetic parameters were calculated according to Eqs. 1-3. IMC_{micro} gel: gel ointment containing IMC microparticles, IMC_{nano} gel: gel ointment containing IMC nanoparticles. The data represent the means ± S.E. of 6 rat skins. *$p < 0.05$ vs. IMC_{micro} gel ointment for each category.

Table 2 Pharmacokinetic Parameters for the In Vivo Percutaneous Absorption of IMC Released from 1% IMC_{micro} and IMC_{nano} Gel Ointments.

Ointment	k_a (h^{-1})	t_{lag} (h)	F	$AUC_{0\text{-}24h}$ (nmol·h/ml)
IMC_{micro} gel	0.39 ± 0.03	0.09 ± 0.01	0.71 ± 0.18	41.3 ± 4.1
IMC_{nano} gel	0.31 ± 0.03	0.08 ± 0.01	0.73 ± 0.20	41.5 ± 3.9

IMC gel ointment was applied to the abdominal skin; the pharmacokinetic parameters were calculated according to Eqs. 4, 5 and 7. IMC_{micro} gel: gel ointment containing IMC microparticles, IMC_{nano} gel: gel ointment containing IMC nanoparticles. The data represent the means ± S.E. of 6 rats.

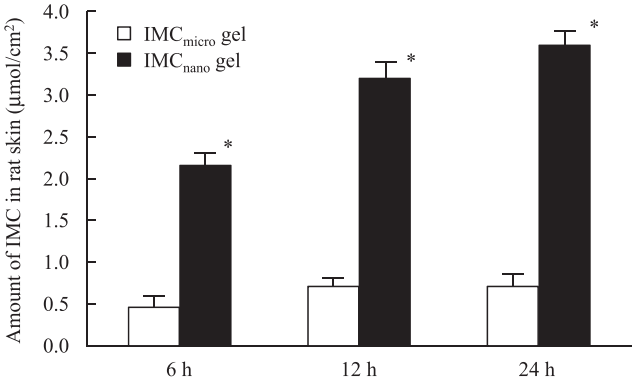

Fig. 5 Amount of IMC in Rat Skin after the Application of IMC_{micro} and IMC_{nano} Gel Ointments.
0.3 g of IMC gel ointment containing micro- (open columns) or nanoparticles (closed columns) was applied to the abdominal skin of rats for 0-24 h. The data represent the means ± S.E. of 6 rats. *$p < 0.05$ vs. IMC_{micro} gel for each category.

ml), and the IMC concentrations in the skin tissue of rats receiving the IMC_{nano} gel ointment were significantly higher than those of rats receiving the commercially available ointment (1.26 ± 0.22 μmol/cm^2, means ± S.E. n = 6 rats). These results suggest that the effects for local therapy are greater following the application of the IMC_{nano} gel ointment than the IMC_{micro} gel ointment or the commercially available IMC gel ointment.

3.2 Therapeutic Effects of IMC_{micro} and IMC_{nano} Gel Ointments on Paw Edema in AA Rats

In studies to develop new topical formulations containing IMC solid nanoparticles for treating RA, the selection of the experimental animal is very important. The AA rat is an animal model in which arthritis is induced by the injection of an adjuvant. Inflammatory pain during the development of AA is assessed by measuring paw edema[50, 51]. Paw edema in AA rats is known to involve two inflammatory processes, primary and secondary inflammation. Primary inflammation starts from the day following the injection of adjuvant into the right hind foot. Secondary inflammation is observed from 7 days after adjuvant injection, and reaches a maximum in both feet 14 days after adjuvant injection into the right and/or left hind foot[4, 52]. It is noteworthy that changes in the biological characteristics of AA rats correspond to those that occur in human RA[4, 50−52]. Therefore, AA rats provide a useful model for use in studies to evaluate transdermal therapeutic systems in RA. Figure 6 and Table 3 show the preventive effects of IMC_{micro} and IMC_{nano} gel ointments on paw edema in AA rats. Paw edema in the right hind foot injected with adjuvant appeared on the day following injection, and reached a maximum after 14 days (Fig. 6A). On the other hand, paw edema of the left hind foot, which was not injected with adjuvant, was not observed during the first 7 days after adjuvant injection, but clearly increased from 10 days, and reached a maximum at 14 days (Fig. 6B). The application of commercially available ointment was significantly prevented the increase in paw edema of the right and left hind feet of AA (right hind feet 29.8 ± 0.85, left hind feet 24.8 ± 0.68, ml·

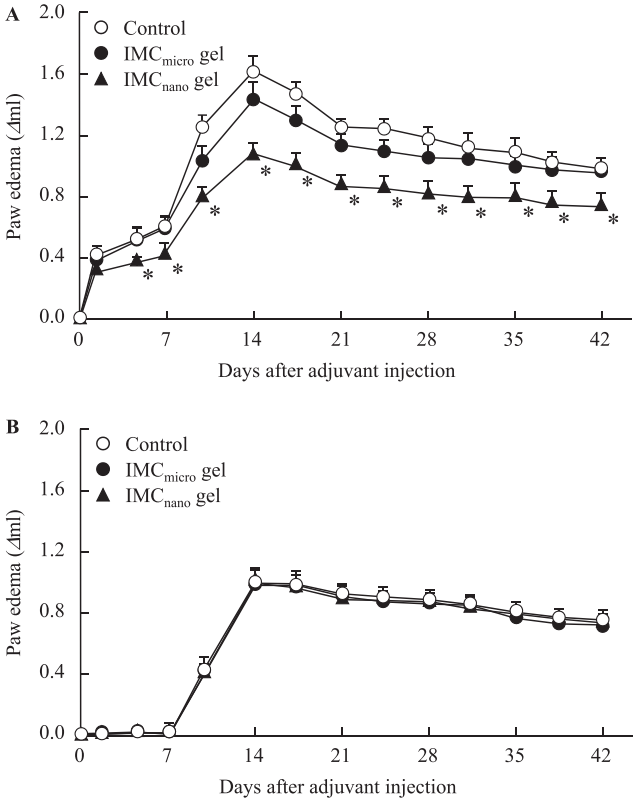

Fig. 6 Changes in Paw Edema of the Right (A) and Left (B) Hind Feet of AA Rats Treated with IMC$_{micro}$ and IMC$_{nano}$ Gel Ointments.
The applications of 0.3 g of gel ointment containing no IMC (control, open circles), or IMC gel ointment containing micro- (closed circles) or nanoparticles (closed triangles) was applied to the right foot once a day (9:00). The data are presented as means ± S.E. of 6 independent rats. *$p < 0.05$ vs. IMC$_{micro}$ gel ointment for each category.

day, means ± S.E. n = 6 rats). This result showed that the increase in plasma IMC concentration caused the suppression of paw edema in both of right and left hind feet. Although, paw edema of the right hind feet of AA rats to which the IMC$_{micro}$ gel ointment was applied tended to be less than, no significant difference was found in comparison with AA rats treated with gel ointment containing no IMC (control gel ointment). In contrast to the results in AA rats treated with the IMC$_{micro}$ gel ointment, paw edema of the right hind feet of AA rats to which the IMC$_{nano}$ gel ointment was less in the days following adjuvant injection, and the $AUC_{0\text{-}42d}$ values were significantly lower than those of AA rats treated with control gel ointment or the IMC$_{micro}$ gel ointment (Table 3). On the other hand, the paw edema of the left hind feet of AA rats to which the IMC$_{micro}$ or IMC$_{nano}$ gel ointment was applied did not differ significantly from

Table 3 Preventive Effects of 1% IMC$_{micro}$ and IMC$_{nano}$ Gel Ointments on Paw Edema in AA Rats.

Ointment	$AUC_{0\text{-}42d}$ (ml·day)	
	Right	Left
Vehicle	48.9 ± 1.9	32.0 ± 1.3
IMC$_{micro}$ gel	45.4 ± 2.1	30.1 ± 1.1
IMC$_{nano}$ gel	32.5 ± 1.7*^{1,2}	31.0 ± 1.0

The values for $AUC_{0\text{-}42d}$ were calculated according to Eq. 8. Vehicle: gel ointment without IMC treated AA rat, IMC$_{micro}$ gel: gel ointment containing IMC microparticles treated AA rat, IMC$_{nano}$ gel: gel ointment containing IMC nanoparticles treated AA rat. The data represent the means ± S.E. of 6 independent rats. *$^{1}p < 0.05$ vs. Vehicle for each category; *$^{2}p < 0.05$ vs. IMC$_{micro}$ gel for each category.

that of rats receiving the control gel ointment. These data suggest that the achievement of relatively high local IMC concentrations in the case of the IMC$_{nano}$ gel ointment resulted in effective therapy.

Further studies are needed to elucidate the precise mechanism for the skin penetration of gel ointments containing IMC nanoparticles. In addition, it is important to clarify a suitable formulation and particle size for a dermal application for RA using IMC particles. Therefore, we are now investigating the therapeutic effects of a topical drug delivery system using IMC particles of various sizes on inflammation and pharmacokinetics in AA rats.

4 CONCLUSIONS

IMC, [1-(4-chlorobenzoyl)-5-methoxy-2-methylindol-3-yl]acetic acid, molecular weight 357.8, pKa 4.5, has been used as therapy for RA patients. However, gastrointestinal lesions are the most common side effect in patients taking IMC, and RA patients taking IMC are more susceptible to IMC-induced gastrointestinal lesions in comparison with other patients[4−8, 11]. Therefore, the development of IMC formulations that do not cause gastrointestinal lesions is highly anticipated. In this study, we have developed a new topical drug delivery system that includes IMC nanoparticles using Bead Smash 12 and additives including HPβCD, MC and Carbopol 934. The accumulation of IMC from the gel ointment in skin tissue and the therapeutic effect on inflammation for the IMC$_{nano}$ gel ointment were significantly greater than those for the IMC$_{micro}$ gel ointment; however, the plasma IMC concentrations were similar between the IMC$_{micro}$ and IMC$_{nano}$ gel ointments. Our findings suggest that a dermal application using nanoparticles may enable a medication to be applied without leading to high systemic levels, providing efficient and effective therapy that spares

patients from unwanted side effects. A formulation of a topical drug delivery system using IMC nanoparticles may provide a delivery option for the clinical treatment of RA.

References

1) Hultqvist, M.; Olofsson, P.; Gelderman, K. A.; Holmberg, J.; Holmdahl, R. A new arthritis therapy with oxidative burst inducers. *PLoS. Med.* **3**, e348(2006).
2) Escandell, J. M.; Recio, M. C.; Manez, S.; Giner, R. M.; Cerda, N. M.; Rios, J. L. Cucurbitacin R reduces the inflammation and bone damage associated with adjuvant arthritis in lewis rats by suppression of tumor necrosis factor-alpha in T lymphocytes and macrophages. *J. Pharmacol. Exp. Ther.* **320**, 581-590(2007).
3) Heyneman, C. A.; Lawless-Liday, C.; Wall, G. C. Oral versus topical NSAIDs in rheumatic diseases: A comparison. *Drugs* **60**, 555-574(2000).
4) Kato, S.; Takeuchi, K. Alteration of gastric ulcerogenic and healing responses in rats with adjuvant-induced arthritis. *Jpn. J. Pharmacol.* **89**, 1-6(2002).
5) Maiden, L.; Thjodleifsson, B.; Theodors, A.; Gonzalez, J.; Bjarnason, I. A quantitative analysis of NSAID-induced small bowel pathology by capsule enteroscopy. *Gastroenterology* **128**, 1172-1178(2005).
6) Kato, N.; Mashita, Y.; Kato, S.; Mitsufuji, S.; Yoshikawa, T.; Takeuchi, K. Sildenafil, an inhibitor of phosphodiesterase subtype 5, prevents indomethacin-induced small-intestinal ulceration in rats via a NO/cGMP-dependent mechanism. *Dig. Dis. Sci.* **54**, 2346-2356 (2009).
7) Kato, S.; Ohkawa, F.; Ito, Y.; Amagase, K.; Takeuchi, K. Role of endothelial nitric oxide synthase in aggravation of indomethacin-induced gastric damage in adjuvant arthritic rats. *J. Physiol. Pharmacol.* **60**, 147-155(2009).
8) Nagai, N.; Fukuhata, T.; Ito, Y.; Usui, S.; Hirano, K. Involvement of interleukin 18 in indomethacin-induced lesions of the gastric mucosa in adjuvant-induced arthritis rat. *Toxicology* **255**, 124-130(2009).
9) Bjarnason, I. Gastrointestinal safety of NSAIDs and over-the-counter analgesics. *Int. J. Clin. Pract. Suppl.* **178**, 37-42(2013).
10) Helleberg, L. Clinical pharmacokinetics of indomethacin. *Clin. Pharmacokinet* **6**, 245-258(1981).
11) Fries, J. F.; Miller, S. R.; Spitz, P. W.; Williams, C. A.; Hubert, H. B.; Bloch, D. A. Toward an epidemiology of gastropathy associated with non-steroidal antiinflammatory drug use. *Gastroenterology* **96**, 647-655 (1989).
12) Ricci, M.; Puglia, C.; Bonina, F.; Di, Giovanni, C.; Giovagnoli, S.; Rossi, C. Evaluation of indomethacin percutaneous absorption from nanostructured lipid carriers(NLC): in vitro and in vivo studies. *J. Pharm. Sci.* **94**, 1149-1159(2005).
13) Consola, S.; Blanzat, M.; Perez, E.; Garrigues, J. C.; Bordat, P.; Rico-Lattes, I. Design of original bioactive formulations based on sugar-surfactant/non-steroidal anti-inflammatory catanionic self-assemblies: a new way of dermal drug delivery. *Chemistry* **13**, 3039-3047 (2007).
14) Kalia, Y. N.; Naik, A.; Garrison, J.; Guy, R. H. Iontophoretic drug delivery. *Adv. Drug Deliv. Rev.* **56**, 619-658 (2004).
15) Denet, A. R.; Vanbever, R.; Préat, V. Skin electroporation for transdermal and topical delivery. *Adv. Drug Deliv. Rev.* **56**, 659-674(2004).
16) Doukas, A. G.; Kollias, N. Transdermal drug delivery with a pressure wave. *Adv. Drug Deliv. Rev.* **56**, 559-579(2004).
17) Mitragotri, S.; Kost, J. Low-frequency sonophoresis: a review. *Adv. Drug Deliv. Rev.* **56**, 589-601(2004).
18) Williams, A. C.; Barry, B. W. Penetration enhancers. *Adv. Drug Deliv. Rev.* **56**, 603-618(2004).
19) Cevc, G. Lipid vesicles and other colloids as drug carriers on the skin. *Adv. Drug Deliv. Rev.* **56**, 675-711 (2004).
20) Delouise, L. A. Applications of nanotechnology in dermatology. *J. Invest. Dermatol.* **132**, 964-975(2012).
21) Gao, X.; Cui, Y.; Levenson, R. M.; Chung, L. W.; Nie, S. In vivo cancer targeting and imaging with semiconductor quantum dots. *Nat. Biotechnol.* **22**, 969-976 (2004).
22) Moghimi, S. M.; Hunter, A. C.; Murray, J. C. Nanomedicine: current status and future prospects. *FASEB J.* **19**, 311-330(2005).
23) Al-Jamal, W. T.; Al-Jamal, K. T.; Tian, B.; Cakebread, A.; Halket, J. M.; Kostarelos, K. Tumor targeting of functionalized quantum dot-liposome hybrids by intravenous administration. *Mol. Pharm.* **6**, 520-530(2009).
24) Boisselier, E.; Astruc, D. Gold nanoparticles in nanomedicine: preparations, imaging, diagnostics, therapies and toxicity. *Chem. Soc. Rev.* **38**, 1759-1782 (2009).
25) Debbage, P. Targeted drugs and nanomedicine: present and future. *Curr. Pharm. Des.* **15**, 153-172(2009).
26) Huang, H. C.; Barua, S.; Sharma, G.; Dey, S. K.; Rege, K. Inorganic nanoparticles for cancer imaging and therapy. *J. Control Release* **155**, 344-357(2011).
27) Huang, X.; Peng, X.; Wang, Y.; Wang, Y.; Shin, D. M.; El-Sayed, M. A.; Nie, S. A reexamination of active and passive tumor targeting by using rod-shaped gold nanocrystals and covalently conjugated peptide ligands. *ACS Nano* **4**, 5887-5896(2010).
28) Ilbasmiş-Tamer, S.; Yilmaz, S.; Banoğlu, E.; Değim, I.T. Carbon nanotubes to deliver drug molecules. *J. Biomed. Nanotechnol.* **6**, 20-27(2010).

29) Chouly, C.; Pouliquen, D.; Lucet, I.; Jeune, J. J.; Jallet, P. Development of superparamagnetic nanoparticles for MRI: effect of particle size, charge and surface nature on biodistribution. *J. Microencapsul.* **13**, 245-255(1996).
30) Begley, D. J. Delivery of therapeutic agents to the central nervous system: the problems and the possibilities. *Pharmacol. Ther.* **104**, 29-45(2004).
31) Bareford, L. M.; Swaan, P. W. Endocytic mechanisms for targeted drug delivery. *Adv. Drug Deliv. Rev.* **59**, 748-758(2007).
32) Dobrovolskaia, M. A.; Aggarwal, P.; Hall, J. B.; McNeil, S. E. Preclinical studies to understand nanoparticle interaction with the immune system and its potential effects on nanoparticle biodistribution. *Mol. Pharm.* **5**, 487-495(2008).
33) Toy, R.; Peiris, P. M.; Ghaghada, K. B.; Karathanasis, E. Shaping cancer nanomedicine: the effect of particle shape on the in vivo journey of nanoparticles. *Nanomedicine(Lond)***9**, 121-134(2014).
34) Misra, R.; Upadhyay, M.; Mohanty, S. Design considerations for chemotherapeutic drug nanocarriers. Pharm. *Anal. Acta.* **5**, 279(2014).
35) Nagai, N.; Ito, Y. Therapeutic effects of gel ointments containing tranilast nanoparticles on paw edema in adjuvant-induced arthritis rats. *Biol. Pharm. Bull.* **37**, 96-104(2014).
36) Cohen, S.; Yoshioka, T.; Lucarelli, M.; Hwang, L. H.; Langer, R. Controlled delivery systems for proteins based on poly(lactic/glycolic acid)microspheres. *Pharm. Res.* **8**, 713-720(1991).
37) Tomoda, K.; Terashima, H.; Suzuki, K.; Inagi, T.; Terada, H.; Makino, K. Enhanced transdermal delivery of indomethacin-loaded PLGA nanoparticles by iontophoresis. *Colloids Surf. B. Biointerfaces* **88**, 706-710 (2011).
38) Tomoda, K.; Terashima, H.; Suzuki, K.; Inagi, T.; Terada, H.; Makino, K. Enhanced transdermal delivery of indomethacin using combination of PLGA nanoparticles and iontophoresis in vivo. *Colloids Surf. B. Biointerfaces* **92**, 50-54(2012).
39) Tomoda, K.; Watanabe, A.; Suzuki, K.; Inagi, T.; Terada, H.; Makino, K. Enhanced transdermal permeability of estradiol using combination of PLGA nanoparticles system and iontophoresis. *Colloids Surf. B. Biointerfaces* **97**, 84-89(2012).
40) Nagai, N.; Ono, H.; Hashino, M.; Ito, Y.; Okamoto, N.; Shimomura, Y. Improved corneal toxicity and permeability of *tranilast* by the preparation of ophthalmic formulations containing *its* nanoparticles. *J. Oleo Sci.* **63**, 177-186(2014).
41) Nagai, N.; Ito, Y. Effect of Solid Nanoparticle of Indomethacin on Therapy for Rheumatoid Arthritis in Adjuvant-Induced Arthritis Rat. *Biol. Pharm. Bull.* **37**, 1109-1118(2014).
42) Nagai, N.; Ito, Y.; Okamoto, N.; Shimomura, Y. A nanoparticle formulation reduces the corneal toxicity of indomethacin eye drops and enhances its corneal permeability. *Toxicology* **319**, 53-62(2014).
43) Franz, T. J. Percutaneous absorption on the relevance of in vitro data. *J. Invest. Dermatol.* **64**, 190-195 (1975).
44) Sloan, K. B.; Siver, K. G.; Koch, S. A. The effect of vehicle on the diffusion of salicylic acid through hairless mouse skin. *J. Pharm. Sci.* **75**, 744-749(1986).
45) Yamaoka, K.; Tanigawara, Y.; Nakagawa, T.; Uno, T. A pharmacokinetic analysis program(multi)for microcomputer. *J. Pharmacobiodyn.* **4**, 879-885(1981).
46) Muller, B. W.; Brauns, U. Solubilization of drugs by modified b-cyclodextrins. *Int. J. Pharm.* **26**, 77-88 (1985).
47) Kristinsson, J. K.; Fridriksdottir, H.; Thorisdottir, S.; Sigurdardottir, A. M., Stefansson, E.; Loftsson, T. Dexamethasone-cyclodextrin-polymer co-complexes in aqueous eye drops. Aqueous humor pharmacokinetics in humans. *Invest. Ophthalmol. Vis. Sci.* **37**, 1199-1203(1996).
48) Nishihata, T.; Kamada, A.; Sakai, K.; Takahashi, K.; Matsumoto, K.; Shinozaki, K.; Tabata, Y.; Keigami, M.; Miyagi, T.; Tatsumi, N. Percutaneous absorption of diclofenac in rats and humans: aqueous gel formulation. *Int. J. Pharm.* **46**, 1-7(1988).
49) Ahmed, T. A.; Ibrahim, H. M.; Ibrahim, F.; Samy, A. M.; Fetoh, E.; Nutan, M. T. In vitro release, rheological, and stability studies of mefenamic acid coprecipitates in topical formulations. *Pharm. Dev. Technol.* **16**, 497-510(2011).
50) Billingham, M. E. Models of arthritis and the search for anti-arthritic drugs. *Pharmacol. Ther.* **21**, 389-428 (1983).
51) Sakuma, S.; Nishigaki, F.; Magari, K.; Ogawa, T.; Miyata, S.; Ohkubo, Y.; Goto, T. FK506 is superior to methotrexate in therapeutic effects on advanced stage of rat adjuvant-induced arthritis. *Inflamm. Res.* **50**, 509-514 (2001).
52) Kato, S. Changes in ulcerogenic response to non-steroidal anti-inflammatory drugs(NSAIDs)in adjuvant arthritic rats. *Yakugaku Zasshi* **121**, 743-751(2001).